Castañeda-Saldarriaga *et al.*
Int J Concr Struct Mater (2021) 15:3
https://doi.org/10.1186/s40069-020-00451-8

International Journal of Concrete Structures and Materials

RESEARCH Open Access

Toward Structural Health Monitoring of Civil Structures Based on Self-Sensing Concrete Nanocomposites: A Validation in a Reinforced-Concrete Beam

Diego L. Castañeda-Saldarriaga[1*], Joham Alvarez-Montoya[1], Vladimir Martínez-Tejada[2] and Julián Sierra-Pérez[1]

Abstract

Self-sensing concrete materials, also known as smart concretes, are emerging as a promising technological development for the construction industry, where novel materials with the capability of providing information about the structural integrity while operating as a structural material are required. Despite progress in the field, there are issues related to the integration of these composites in full-scale structural members that need to be addressed before broad practical implementations. This article reports the manufacturing and multipurpose experimental characterization of a cement-based matrix (CBM) composite with carbon nanotube (CNT) inclusions and its integration inside a representative structural member. Methodologies based on current–voltage (I–V) curves, direct current (DC), and biphasic direct current (BDC) were used to study and characterize the electric resistance of the CNT/CBM composite. Their self-sensing behavior was studied using a compression test, while electric resistance measures were taken. To evaluate the damage detection capability, a CNT/CBM parallelepiped was embedded into a reinforced-concrete beam (RC beam) and tested under three-point bending. Principal finding includes the validation of the material's piezoresistivity behavior and its suitability to be used as strain sensor. Also, test results showed that manufactured composites exhibit an Ohmic response. The embedded CNT/CBM material exhibited a dominant linear proportionality between electrical resistance values, load magnitude, and strain changes into the RC beam. Finally, a change in the global stiffness (associated with a damage occurrence on the beam) was successfully self-sensed using the manufactured sensor by means of the variation in the electrical resistance. These results demonstrate the potential of CNT/CBM composites to be used in real-world structural health monitoring (SHM) applications for damage detection by identifying changes in stiffness of the monitored structural member.

Keywords: smart materials, structural health monitoring, self-sensing, carbon nanotubes, cementitious composites, nanocomposites, civil structures

1 Introduction

It is a fact that materials and structures degrade with time and usage. Within the context of civil structures (e.g., buildings, bridges, tunnels, dams, among others), natural and human-made hazards (e.g., earthquakes, typhoons, hurricanes, fire, or collisions) represent also threats to the structural integrity that may cause catastrophic failures involving economic and human losses Xu and He (2017). This requires the implementation of inspection procedures to guarantee serviceability and

*Correspondence: dcastan93@gmail.com
[1] Grupo de Investigación en Ingeniería Aeroespacial (GIIA), Escuela de Ingenierías, Universidad Pontificia Bolivariana, 050031 Medellín, Colombia
Full list of author information is available at the end of the article
Journal information: ISSN 1976-0485 / eISSN 2234-1315

reliability of structures in their long lifetimes. These inspections are often carried out at a fixed time intervals using different methods comprised within the field of nondestructive testing (NDT), where the quality or integrity of a component is determined nondestructively by interrogating one or several physical variables that are damage-sensitive Shull (2002).

Some NDT methods include visual testing (both direct and remote) Agnisarman et al. (2019), ultrasonics Zhao et al. (2018), acoustic emissions Meo (2014), infrared thermography Yamazaki et al. (2018), ground penetrating radar techniques, and electrical resistivity tomography Salin et al. (2018). These methods commonly require human intervention that increases uncertainty and implies costly equipment and personnel. SHM overcomes these factors using approaches where sensors are permanently installed into the structure, so that NDT is performed continuously or online Xu and He (2017). In this regard, SHM can reduce costs by providing valuable information for maintenance management, improve reliability by the possibility of finding damages at incipient stages, and improve future designs by making available valuable information about the performance of the current ones Ogai and Bhattacharya (2018).

Recent advances in SHM for civil structures include the use of piezoelectric sensors Liao and Chiu (2019), fiber-optic sensors (FOS) Glisic et al. (2013), Barrias et al. (2019), Xu et al. (2019), electrochemical sensors (e.g., potentiometric, amperometric, and conductometric) Hu et al. (2011), Qiao et al. (2012), and self-sensing composite materials Tian et al. (2019). A deep review of the sensing technologies applied to civil structures was recently reported by Taheri (2019). Considering the available sensing technologies, one concern when developing effective SHM systems is the selection of the type of sensor to be used. The resistance and durability of the sensor operating in harsh environments and its integrability to large structures are paramount. That is why, self-sensing composites, materials that not only bear loads but provide measures as a response to an external stimulus, have raised the interest of the research community (D'Alessandro et al. 2016a; Han et al. 2015a; Rana et al. 2016; Yang et al. 2020).

As cement-based materials or cementitious composites (e.g., paste, mortar, and concrete) are the most popular building materials Xu and He (2017), much of the scientific research around self-sensing composites is related to such materials. Self-sensing cementitious composites, also known as smart concretes, are fabricated by mixing functional fillers (e.g., carbon fibers Baeza et al. 2013; Teomete 2015; Sarwary et al. 2019, carbon nanotubes Elkashef 2015, steel fibers Kang et al. 2018; Ding et al. 2019, graphite powder Šimonová et al. 2018, nickel powder Wang et al. 2015 , among others Tian et al. 2019). Particularly, CNTs have raised the interest in the last years due to their high specific mechanical and transport properties (Schumacher and Thostenson 2014; Ubertini et al. 2016).

The incorporation of CNTs in cementitious materials can endow these materials with a piezoresistive behavior. The CNTs are materials that, when subjected to strain, their electrical properties change up to two orders of magnitude, exhibiting a proportional and reversible piezoresistive response to the external stimulus (Garcia-Macias et al. 2017; García-Macías et al. 2017; Minot et al. 2003). This electromechanical behavior is explained first by various authors as a change in the conductivity of the CNT due to the change in the energy band induced by the strain applied on its volume (Minot et al. 2003; PHAM 2008; Han et al. 2015b; Njuguna 2012; Tjong 2009; Xinxin Sun 2009).

Second, as the matrix is dielectric, electrical properties are filler-dominated by the CNT networks and the composite's electrical conductivity changes according to the strain conditions Tian et al. (2019). In other words, by adding conductive fillers in dielectric matrices such as CNTs, there is a change in conductivity proportional to the CNT concentration. Under the application of load due to strain, the CNT network changes as well as overall conductivity. In this way, concretes with CNTs as fillers can be used as strain sensors. Moreover, such composites can also be used for damage detection, since CNT networks can also be disturbed by damages such as cracks.

Despite this approach is promising for SHM of civil structures and different studies have been conducted in the field, including electromechanical characterization (Ubertini et al. 2014; Meoni et al. 2018; Liu et al. 2019; Kim et al. 2019), fabrication procedures (D'Alessandro et al. 2016a; PParvaneh and Khiabani 2019), and modeling techniques (Garcia-Macias et al. 2017; Eftekhari et al. 2014; García-Macías et al. 2018), it is still considered in their infancy stage. A broad practical implementation is still not possible at the moment Taheri (2019).

There are some issues that need to be addressed before a wide implementation of this technology in infrastructures, such as quality and variability in fabrication, uniform dispersion of fillers in the matrix, measurement procedures allowing reliable, and repeatable monitoring of conductivity and approaches to damage detection in full-scale civil engineering structures (Tian et al. 2019; D'Alessandro et al. 2016b; Shi et al. 2019).

Compared with characterization and fabrication, little research has been conducted to investigate the integrability and damage monitoring capabilities of self-sensing cementitious composites in structural members made

of reinforced concrete under complex load scenarios as expected in real-world modern infrastructures (Lagason et al. 2016; You et al. 2017; Al-Dahawi et al. 2017; Naeem et al. 2017). Damage monitoring in beams or columns greatly depends on the self-sensing composite configuration.

Most of the reported studies have proposed the construction in bulk, namely, the whole member is made of the self-sensing composite providing higher sensitivity to damages (Hannan et al. 2018; Lagason et al. 2016; Al-Dahawi et al. 2017; Downey et al. 2017a; Gupta et al. 2017; You et al. 2017; Yıldırım et al. 2018). For example, Al-Dahawi et al. (2017) fabricated engineered cementitious composites with different carbon-based materials, including CNTs. Then, the beam specimens were loaded under four-point bending tests in the elastic and plastic regions to sense damage. The results were suitable in the plastic region; however, upon unloading in the elastic region, the authors found not successful results.

Downey et al. (2017b) developed a resistor mesh model to detect, localize, and quantify damage in structures from self-sensing cementitious composites based on the hypothesis that the electrical resistance of any self-sensing conductive material depends on its strain and damage states. Yıldırım et al. (2018) investigated the self-sensing capabilities of reinforced large-scale beams designed to fail under shearing in four-point bending tests. The authors successfully proved that increments in maximum shear crack width produce changes in the electrical resistance.

Nevertheless, when dealing with a practical implementation of such bulk fabrication, which often requires demanding laboratory procedures, it does not seem cost-effective toward a broad implementation. Other alternatives include coatings (Downey et al. 2017b, 2018; Nešpor and Nejedlík 2018), in which one surface of the member is covered with a layer of the self-sensing composite, embedded Meoni et al. (2018); Saafi (2009); D'Alessandro et al. (2017), where the self-sensing composite is prefabricated into standard small-size sensors and then integrated into the member, and novel forms dealing with coatings aggregates (Han et al. (2015c); Gupta et al. (2017); Loh and Gonzalez (2015)).

The embedded form has the advantage of being less expensive and easier to integrate for practical applications. Civil structures can be designed with a network of such sensors to allow distributed sensing over large areas without needing a high amount of material and disturbing the structural performance. Additionally, this form is suitable for SHM of existing infrastructure as opposed to the bulk form, which may be restrained to new constructions.

Saafi (2009) proposed CNT/cement sensors embedded into concrete beams for crack detection under three-point bending tests. The authors demonstrated that sudden changes in the electrical resistance are indicative of crack initiation. D'Alessandro et al. (2016c) embedded cement-based sensors doped with CNTs for strain monitoring of reinforced-concrete beams. The authors proposed a damage detection strategy based on vibration tests carried out by exciting the beam with a hammer. Spectral analysis of the results obtained with the smart sensors and with strain gauges included for validation demonstrated similar results; therefore, vibration-based SHM is feasible with these sensors. Lim et al. (2017) performed crack onset monitoring by embedding cementitious composite sensors in reinforced mortar beams. The authors based their damage detection strategy on the fact that if the cracks nucleate in the concrete, it could be propagated to the sensor and, therefore, the conductivity will change. Naeem et al. (2017) evaluated the feasibility of crack sensing using CNT/cement composites in reinforced mortar beams. The authors found that steep changes in the resistance occurred at failure of the mortar under flexural loading.

The damage detection approaches reviewed above rely on damages or cracks propagating to the cementitious composite sensors to change the CNT network and, hence, change resistance measurements. However, in real scenarios, non-allowable damages may not penetrate the sensor leading to misclassifications. Based on previous work related to strain-based SHM (Sierra-Pérez et al. 2018; Sierra-Pérez and Alvarez-Montoya 2020), it is proposed to use resistance measurements (correlated with strain measurements) to detect damages relying on that a damage occurrence (e.g., cracks, inclusions, corrosion, among others) affects the local stiffness of the structure and, therefore, the strain field is modified.

The aim of this paper is to present a multipurpose study that includes the characterization of cementitious composites with inclusions of CNTs, different test procedures, and a proof-of-concept demonstration in a simply supported beam made of reinforced concrete of the suitability of these types of sensors for strain-based SHM. The novelty of this study focuses on the effective integration of the self-sensing concrete sensors in a structural member and in using information from them for damage detection based on strain, demonstrating their suitability for future practical SHM applications.

This paper is divided into four sections, after this brief introduction, the experimental procedures to develop the specimens under study, and their characterization methods, including I–V obtaining curves, DC-based electrical characterization, and characterization of piezoresistive behavior. After that, the results

of such characterizations are shown in conjunction with the proof-of-concept in the structural member for SHM purposes.

2 Experimental Procedure

The experimental procedure used in this work was divided into two parts: the first one is focused on the dispersion of CNTs into a cement-based matrix (CBM), having as a main objective to obtain a uniform distribution of CNTs within the matrix. The second part deals with the electromechanical behavior and topographic characterization of the CBM/CNT, using a scanning electron microscopy (SEM) and DC/BDC methodologies.

2.1 CNT Dispersion and Sample manufacturing

For the CBM, Portland cement, quartz sand, and water were used, in a water-to-cement ratio of 1:3 following standard ASTM C109 (2000). The CNTs used in this work were multiwalled type, from 10 to 20 micrometers in length and 50 to 80 nanometers in diameter supplied by Nanostructured and Amorphous Materials, Inc.

As dispersing agent, sodium dodecyl sulfate (SDS) was used to avoid the agglomeration of CNTs within the CBM, to improve the dispersion quality, and to increase the concrete workability. In previous works (Castaneda-Saldarriaga et al. 2019; Kyrylyuk and van der Schoot 2008; Shao et al. 2017; Myung et al. 2014; Sasmal et al. 2017; Rehman et al. 2018), dispersants such as Triton X-100, Tween 20, and SDS were evaluated to determine the proportion and mixtures that improved the CNT dispersion. These studies concluded that SDS is the most suitable in terms of avoiding the agglomeration of CNTs.

To estimate what percentage above the percolation threshold (defined as the minimum fraction of CNTs necessary for the material to exhibit electrical conductivity) generates better piezoresistive properties, CNT percentages by weight (%*wt*) of 0.2, 0.5, and 0.8 of the CBM were selected following the experimental methodologies proposed in the literature (Coppola et al. 2011; Downey et al. 2017a; Cui 2013; Garcia-Macias et al. 2017; Baeza et al. 2013; Yoo et al. 2018).

Since the piezoresistive effect considerably depends on a proper CNT dispersion and these tend to agglomeration due to Van der Waals forces, the used methodology started by preparing a solution of SDS dispersant with a water-to-dispersant ratio of 10:1 (Shao et al. 2017; Noh et al. 2013; Lee and Park 2017; Collins et al. 2012). To obtain the water/dispersant solution (see Fig. 1a), a BRANSON S-450D ultrasonic sonicator with a maximum power of 400 Watts and a tip of 6.35 mm was used for 5 min (1 s on and 2 s off, so that overheating the sample was avoided) (Konsta-gdoutos et al. 2010; Konsta-Gdoutos and Aza 2014). Once a solution between water and dispersing agent was obtained, the different proportions of CNTs were added to the solution and the ultrasonic sonicator was used for another 45 min in the same configuration (Fig. 1b). The ultrasonic sonicator power was set at 12 W for both processes.

Simultaneously, according to the ASTM C109 standard and Qiao et al. (2012), the quantities of sand and cement for the manufacture of concrete samples (as shown in Fig. 1c) were mixed with a mechanical stirrer. The next step was to pour the water/dispersant/CNTs solution into the cement/sand mixture. Thereupon, the mixture was homogenized using a mechanical stirrer at a constant speed of 200 rpm (Fig. 1d) following ASTM C1329 and ASTM C109 standards (Collins et al. 2012; American Society for Testing and Materials 2014).

Finally, the CBM/CNT composite was cast in cube molds of $52 \times 52 \times 52$ mm, following ASTM C109 ASTM C109 (2000) (Fig. 1e), whereby copper electrodes were arranged in mesh-like configuration (as shown in Fig. 2), so that it was embedded in the material. Copper was selected as the electrode material due to its low electrical resistance, which guarantees that the obtained electrical resistance measurements of the composite material mostly belong to the material and not to the electrodes Kim et al. (2016). All CBM/CNT samples were naturally aged for 28 days under ACI 308 standard ACI Committee 308 (2016).

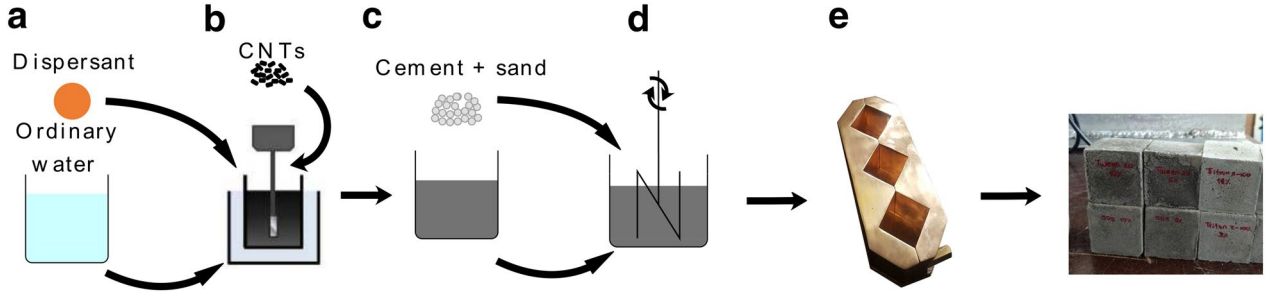

Fig. 1 Manufacturing process of the CBM/CNT composites.

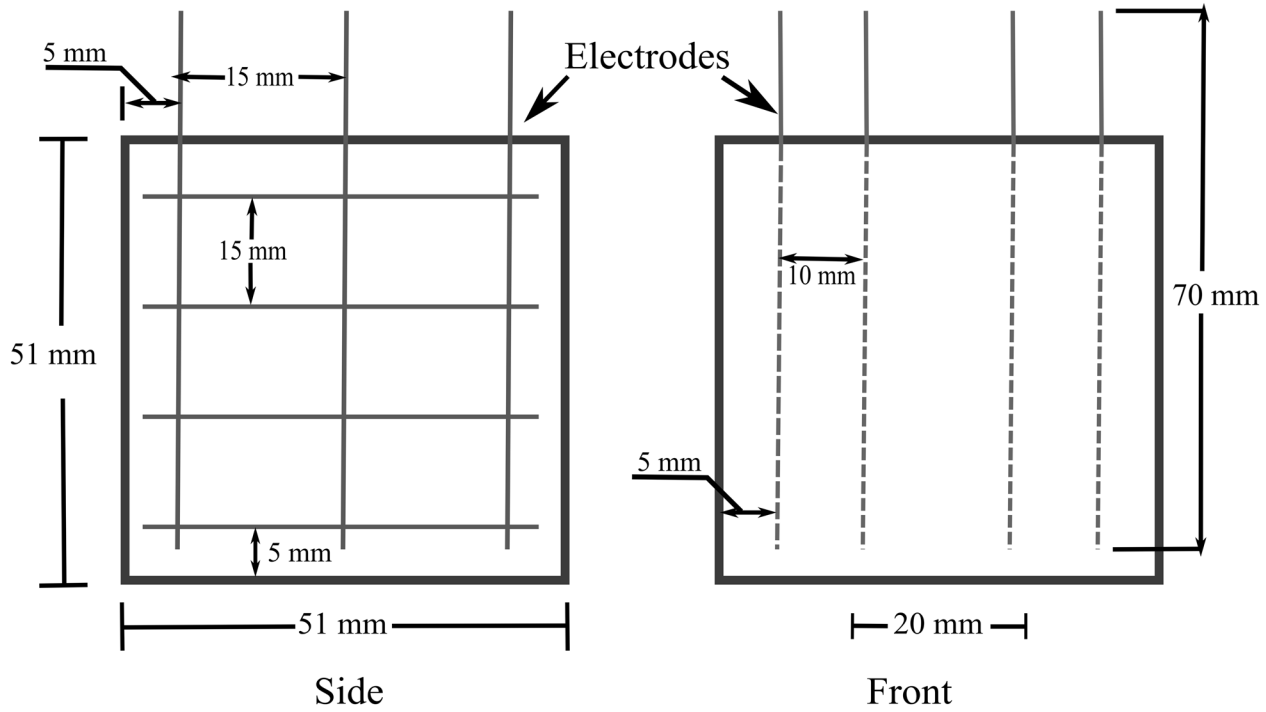

Fig. 2 CBM/CNT specimens and copper electrodes mesh-type configuration.

2.2 Electrical and Topographic Characterization of the CBM/CNT Material

The topographic images of the CBM/CNT were obtained to analyze the CNT dispersion within the CBM; for this purpose, an SEM was used. To characterize the Ohmic behavior of the CBM/CNT composite, an I–V curve test was implemented following the work performed by Han et al. (2015a). This characterization helps to select the suitable measuring method and the measuring equipment. A comparison was also carried out between the use of techniques that involve direct current (DC) to find an appropriate methodology to measure the electrical properties of the CBM/CNT materials. Finally, the methodology used to characterize the self-sensing phenomenon in CBM/CNT and RC beam is presented.

2.2.1 Scanning Electron Microscopy of CBM/CNT Material

After aging, specimens with different concentrations of CNTs were characterized using SEM. A Jeol JCM-6000 SEM was used to find a relationship among the concentration of CNTs, its dispersion, and the electrical resistance of each specimen. A thin gold/palladium coating was deposited on the surface of the samples to avoid overload phenomena in dielectric samples when they are irradiated with the electron beam.

2.2.2 Ohmic Characterization of the CBM/CNT Material

Characterizing the Ohmic behavior of the material involves measuring its amperometric response when a voltage (V) input is applied in order to obtain the I–V curves. For this purpose, a typical assembly of an ammeter, a DC power supply, and a 10 kOhm resistor were used for obtaining I–V curves of each specimen Yorke (1981).

I–V curves were obtained by sequential voltage increase applied between the electrodes and measuring the current change through the CBM/CNT. Measuring the Current through the CBM/CNT required an electrical resistor in series with one of the CBM/CNT electrodes as is shown in Fig. 3a. Afterward, a UNIT-T digital multimeter model UT39A was used to measure the current flowing through the specimen. The applied electrical voltage ranges from 0 to 9 volts with 0.5 V steps. Three sequential repetitions were performed for each sample.

2.2.3 Electrical Resistance Characterization of the CBM/CNT Using DC and BDC Procedures

Once the Ohmic behavior was validated by means of the analysis of the I–V curves, DC and BDC methodologies were implemented to characterize the CBM/CNT electrical resistance. The experimental setup for the electrical resistance measurement using DC required only a digital multimeter (Fluke model 112), as shown in Fig. 3b.

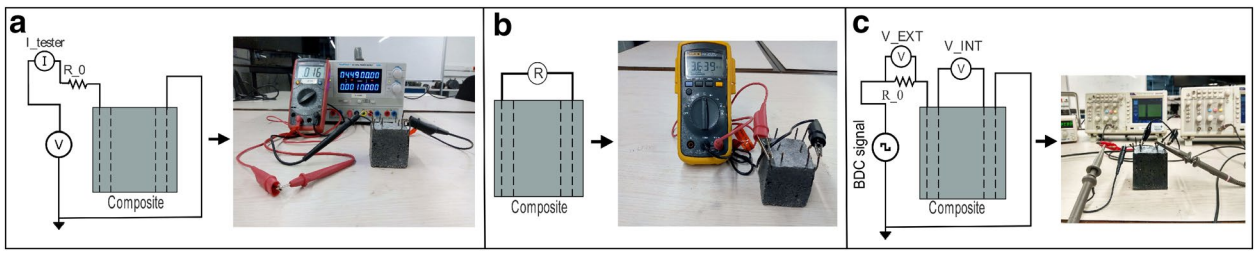

Fig. 3 **a** Electrical connection diagram for ohmic characterization of the CBM/CNT. **b** Electrical connection diagram for characterization of the electrical resistance using DC source. **c** Electrical connection diagram for characterization of the electrical resistance using BDC.

Sampling rate frequency was set in 1 Hz (Downey et al. 2017b; Coppola et al. 2011; Dong et al. 2016).

On the other hand, BDC was selected to avoid the polarization effect generated by the modification of the charge distribution that occurs in dielectric materials when an electric field is applied. BDC uses a square DC wave responsible for discharging the molecules applying an electronic flow in the opposite direction to the power supply voltage (Downey et al. 2017a; Böttcher 1973).

The methodology for CBM/CNT electrical resistance measuring using BDC was proposed by Downey et al. (2017a). According to the authors, a four-probe method type assembly is recommended. For this purpose, a two-phase DC source with a 50% duty cycle square wave output signal was used. To perform the electrical characterization using BDC, a 5 V peak–peak voltage between the specimen electrodes V_{EXT} was applied with 1 Hz wave frequency. To measure the voltages (V_{EXT} and V_{INT}), two Tektronix brand oscilloscopes (model TDS 1012C - EDU) were used, with a resolution of 0.02 V at a data sampling rate of 1 Hz. Only the positive values of the square signal supplied to the circuit were taken. A R_0 resistor of 1 kOhm was connected in series to the circuit to determine the current flowing through the CBM/CNT, as is shown in Fig. 3c.

Finally, to determine the electrical resistance of the composite material, the average value of V_{EXT} set in the 80% of the positive wave was taken and multiplied by R_0 using Ohm's law, finding in this way, the current (I) flowing through the CBM/CNT. Then, the average value of V_{INT} set in 80% of the positive wave was taken and divided by the current (I), finding the resistance of the CBM/CNT.

2.2.4 CBM/CNT Piezoresistive Behavior Characterization

To evaluate the electrical and mechanical behavior of the CBM/CNT material, the electrical resistance was measured, while a uniaxial compressive test was carried out using an INSTRON 5582 universal testing machine (see Fig. 3b). Each specimen was instrumented with a Fiber Bragg Grating (FBG) bonded on the surface of one of the faces of the CBM/CNT subjected to compression to measure strain. A fiber-optic interrogator (Micron Optics SM130-700) was used for acquiring the wavelength shift as a function of a mechanical stimulus applied to the CBM/CNT. The electrical resistance and strain values were acquired at a frequency rate of 1 Hz.

The maximum magnitude of the applied load applied was 5 kN. No more than 120 $\mu\epsilon$ were obtained for any measurement. This strain level ensures no damages in the CBM/CNT specimens taking into account the Young's modulus and strength of the Portland cement used. Figure 4 shows the experimental setup used for the piezoresistive characterization of the material.

To correlate the variation of the electrical resistance and the strain, the expression described in Eq. 1 was used:

$$\lambda = \frac{\Delta R}{\epsilon R}, \tag{1}$$

where R is the initial resistance, ΔR is the difference between initial resistance and final resistance, and ϵ are the strain measured by the FBG (Pisello et al. 2017; Jang et al. 2017).

2.2.5 Health Monitoring of a Reinforced-Concrete Beam Using the CBM/CNT Material

Once the CBM/CNT piezoresistive behavior was characterized, a CBM/CNT was embedded into an RC beam to assess its self-sensing response. For this purpose, a CBM/CNT coupon was made using the same experimental procedure related in Sect. 2.2.3 but having a different geometry (i.e., parallelepiped instead of a cube).

To ensure the load transfer between the RC beam and the CBM/CNT, corrugated steel rods (dowels) of 6.35 mm diameter and 80 mm length were used (Fig. 5a). Half of its length was embedded into the CBM/CNT parallelepiped and the remaining into the RC beam, as can be seen in Fig. 5c. The central section of the CBM/CNT

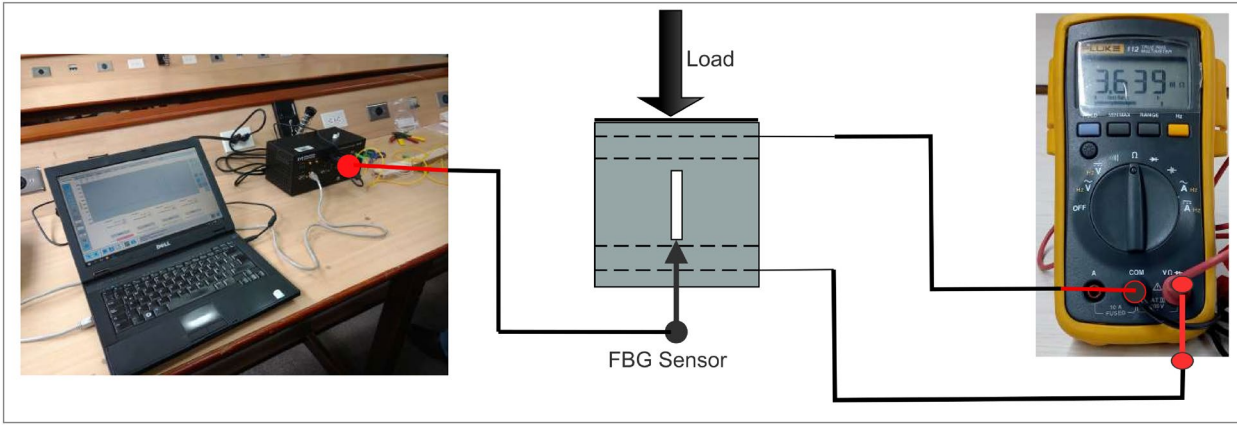

Fig. 4 Experimental setup for CBM/CNT piezoresistivity determination.

Fig. 5 RC-beam manufacturing for the validation of the sensor operation for health monitoring. **a** CBM/CNT parallelepiped with corrugated steel rods. **b** Inclusion of the CNC/CBM parallelepiped within the steel frame of the RC beam. **c** Casting over the CNC/CBM parallelepiped and the reinforced steel structure of the concrete for the fabrication of the RC beam.

coupon remains without corrugated steel rods as seen in Fig. 5a.

In this way, besides the chemical bond which serves as interface between the concrete and corrugated steel, a mechanical bonding occurs between both of them. Therefore, the load transfer between the concrete beam and the CBM/CNT occurs through both effects.

To guarantee that the electrical properties of the CBM/CNT parallelepiped with corrugated steel rods did not differ from those exhibited by the specimens made by following ASTM C109 standard ASTM C109 (2000) described in Sect. 2.1, the following steps were adopted:

- The same proportion of CNT and dispersion method were used, as well as the same proportions of cement, water, sand, and dispersant.
- The distance between the electrodes in the middle volume of the parallelepiped was ensured to be the same as that used in the specimens described in 2.1.
- The dimensions of the cross-section of the parallelepiped remained the same as those of the specimens described in Sect. 2.1 and the measurements of the copper electrodes in mesh-type configuration were the same, as shown in Fig. 2.

The RC beam (where the CBM/CBM parallelepiped was embedded) was made of the same structural materials and proportions used to make the CBM, as described in Sect. 2.1 (see Fig, 5b) but without the addition of CNTs. Its final dimensions were 650 mm in length, with a cross-section of 160×130 mm.

The integration of the CBM/CNT parallelepiped within the RC beam was carried out by positioning the specimen in the steel frame, as shown in Fig. 5b. Hereinafter, the steel frame and CBM/CNT parallelepiped were placed in a wood formwork where the concrete was cast. Finally, the RC beam was aged for 28 days.

For the validation of the CBM/CNT parallelepiped embedded within the RC beam as a strain sensor, a three-point bending test was performed. The distance between supports was set in 600 mm and a dynamic load was applied to the RC beam from 0 to 14 N at a constant displacement

speed of 5 mm/min. Measurements of the electrical resistance of the CBM/CNT were taken while applying load using the same methodology described in the previous section. The experimental setup can be seen in Fig. 6.

One alternative in SHM based on strain measurements is to study the slope changes in a load–strain curve (which represents the global stiffness of the RC beam) promoted by damage occurrence. An actual damage (e.g., a crack) reduces the global stiffness, and therefore, the slope of the curve decreases. On the other hand, a positive damage increases the global stiffness and the slope should increase.

To infer changes in the global stiffness of the RC beam, it was necessary to create a baseline for the pristine condition. A baseline is an accurate measurement of a process functionality before any change of an input variable occurs. These data allow comparing the effect of a change in the behavior of the phenomenon being evaluated. The baseline for the pristine beam was built by using the aforementioned load conditions.

After building the baseline for the RC beam, a positive artificial damage (addition of stiffness to the cross-section) was induced on it. In this sense, a steel plate was adhered to one of the beam surfaces to increase the stiffness of the cross-section by 20%. The dimensions of the steel plate were 160 × 160 mm and 10 mm thick.

The steel plate was bonded to the surface using an epoxy adhesive, for which it was necessary to prepare both surfaces by an abrasive process (to flatten the surface) and cleaning (to remove dirt and rust). Afterward,

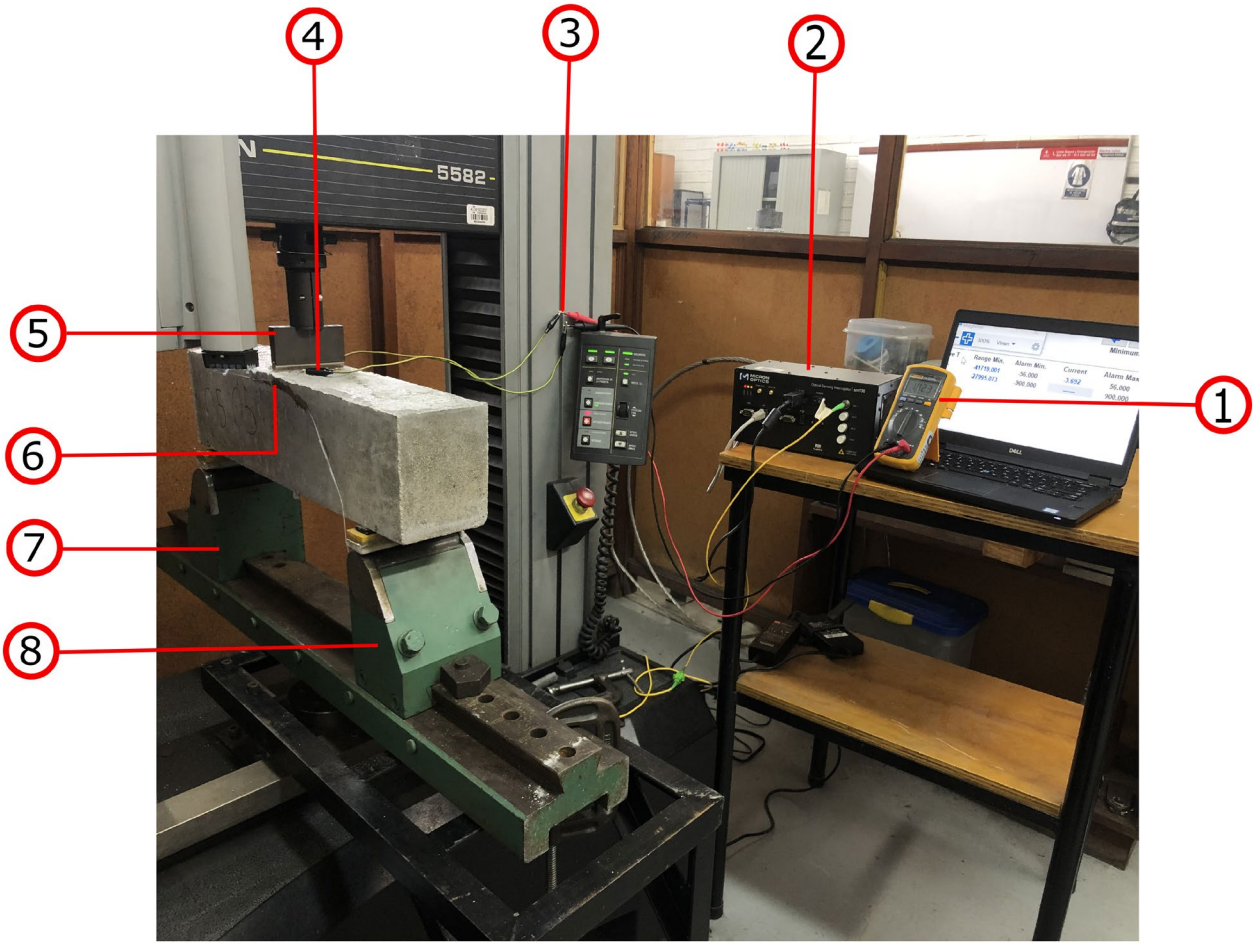

Fig. 6 Experimental setup: RC beam in INSTRON universal testing machine with 100 kN load cell, in the configuration for bending test. 1) Fluke 112 multimeter. In this assembly, it is used to measure the electrical resistance of the self-sensing material. 2) Micron Optics SM130 fiber-optic interrogator. This equipment was used to obtain strain data from the FBG. 3) Connection of the tips of the digital multimeter with the electrodes of the self-sensing material. 4) Cementitious matrix sensor electrodes. 5) Load cell support on the beam. 6) FBG sensor positioned, so that the compression to which the sensor is exposed is measured when a load is applied to the beam. 7 and 8) Supports for three-point bending measurement.

to keep the steel plate in contact with the RC beam, while the epoxy adhesive cured, "C-clamps" were used.

Same load conditions used for the pristine condition were used for testing the "damaged" RC beam. Data for the variation of the electrical resistance of the CBM/CNT parallelepiped were acquired, whilst load was applied. The experiments for the pristine and damaged states were repeated ten times each. The experimental setup shown in Fig. 3b was implemented to measure the variation of the electrical resistance for both states (pristine and damaged).

3 Results and Discussion

3.1 Image Analysis of the CNT Dispersion Within the CBM

Results from SEM images at a 10 μm scale are presented in Fig. 7. As expected, the growth of agglomerations or clusters of CNTs within the CBM decrease as the %*wt* of CNT increases, as can be seen from Fig. 7a–c. This result entails that as the CNT percentage within the sample increases, the distribution of CNTs within the sample tends to become uniform, since CNT agglomerations generate larger clusters that cover larger areas, producing a uniform lattice within the entire composite (Garcia-Macias et al. 2017; Nam and Lee 2015).

In Fig. 7a, it can be observed that CNTs are agglomerated in a few clusters. Also, these are randomly scattered on the surface and distant from each other, so it is estimated that the electrical conduction phenomenon occurs mostly by electron hopping (Balberg et al. 1984; Garcia-Macias et al. 2017), and consequently, this sample is below the percolation threshold.

Figure 7b shows CNT clusters homogeneously distributed. Additionally, the distance among clusters decreases compared with Fig. 7a, and it can be expected that the electrical conductivity phenomenon occurs both by electron hopping and by conductivity networks among CNTs. This behavior indicates that the sample with 0.5 %*wt* is above the percolation threshold (Balberg et al. 1984; Garcia-Macias et al. 2017).

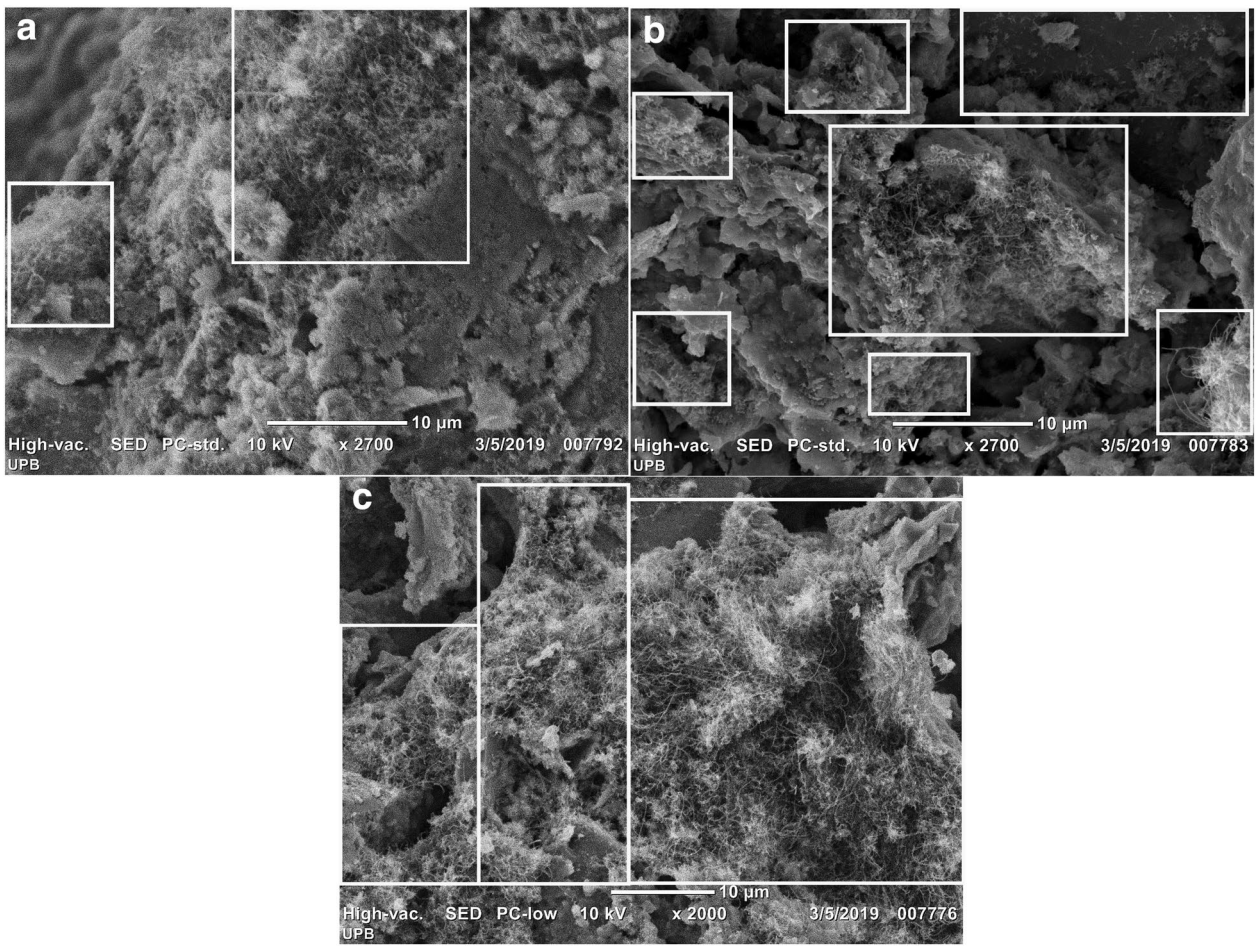

Fig. 7 SEM images for samples: **a** 0.2 %*wt* (2700X), (**b**) 0.5 %*wt* (2700X) and (**c**) 0.8 %*wt* (2000X).

Furthermore, observing Fig. 7c, it can be seen that there is no significant difference or separation between the CNT clusters when the sample has 0.8%*wt*, so it can be affirmed that this sample is above the percolation threshold. Accordingly, it can be estimated that the qualitative results presented in Fig. 7 allow the percolation threshold to be estimated between 0.2 %*wt* and 0.5 %*wt* for this type of composite as was reported by Souri et al. (2017), Garcia-Macias et al. (2017), and Hoseini et al. (2017).

None of Fig. 7b and c exhibited isolated clusters, which are signs of issues caused by agglomeration associated with a poor CNT dispersion within the CBM (Nam and Lee 2015; Wang et al. 2015). Hence, it can be affirmed that the CNT dispersion inside the samples with 0.5 %*wt* and 0.8 %*wt* is homogeneous.

Finally, the images shown in Fig. 7 allow proposing two hypotheses regarding the implemented manufacturing method:

- There is a uniform distribution of CNTs within the cementitious matrix, at least for samples with 0.5 and 0.8 %*wt*, validating the proportions of the constituents selected to make the CBM/CNT material and, in general, the methodology used to disperse the CNTs within the CBM.
- The higher the CNT fraction, the greater the number of clusters that are close to each other, and, therefore, greater the number of CNTs in contact, which entails a greater electrical conductivity.

3.2 Ohmic Characterization of the CBM/CNT

The Ohmic behavior of the material was studied using the I–V curves described in Sect. 2.2.2 and schematized in Fig. 3a. From Fig. 8a–c, it is shown the amperometric response (I–V curves) of the CBM/CNT when an electrical potential is applied. These figures showed a linear relationship between voltage and current; therefore, it is concluded that the CBM/CNT material having 0.2, 0.5, and 0.8 %*wt* exhibits an electrical behavior equivalent to an ideal resistor. From this result, it was determined that any technique or methodology for characterizing the electrical resistance that assumed the material behavior as an Ohmic material can be implemented.

An approximate measure of the electrical resistance of obtained for each specimen using I–V curves and Ohm's law is presented in Table 1. Nevertheless, the electric resistance measurements of the samples with 0.2 and 0.5 %*wt* of CNTs presented a high standard deviation, which implies low reliability, concluding that it is necessary to

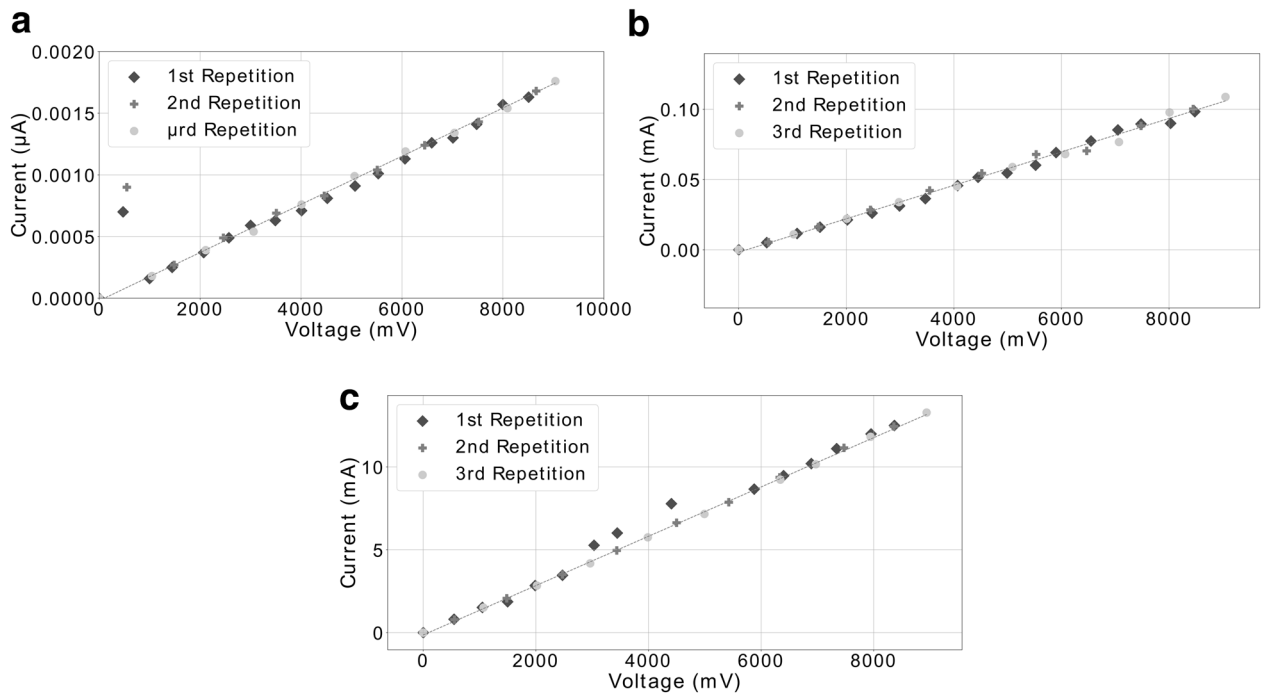

Fig. 8 Curves I–V using DC for samples with (**a**) 0.2 %*wt* of CNTs, **b** 0.5 %*wt*, and **c** 0.8 %*wt*.

Table 1 Electrical resistance values and their corresponding standard deviations obtained from the I–V curves characterization.

CNTs (%*wt*)	Average electrical resistance (Ω)	Standard deviation (Ω)
0.2	5335505.50	250871.25
0.5	88245.70	3813.08
0.8	693.32	14.99

implement measurement methods with higher accuracy. Moreover, it can be seen a change up to four orders of magnitude in the value of electrical resistance when the fraction of CNTs increases from 0.2 to 0.8 %*wt*, exposing that the percolation threshold is between 0.2 and 0.8 %*wt* as also reported by Garcia-Macias et al. (2017).

3.3 Electrical Resistance Characterization of the CBM/CNT Using DC/BDC Methodologies

Results showed in Fig. 9 were obtained following the experimental setup for electrical characterization. Around this figure, an analysis is presented regarding the relevance of methodologies based on DC and BDC sources against the decrease in data dispersion.

It can be seen that the electric polarization phenomena appear when measurements are made using DC methods for 0.2 %*wt* and 0.5 %*wt*. Figure 9a shows a constant increase of the electrical resistance against the time; these phenomena do not tend to stabilize before 40 s. Likewise, Figure 9a also exhibits electrical polarization; however, it tends to stabilize after 40 s.

The polarization phenomena in the CBM/CNT material with 0.2 %*wt* and 0.5 %*wt* are due to the dielectric nature of the matrix and the low CNT concentration. To explain the polarization phenomena presented in CBM/CNT, it is necessary to consider that the electrical behavior of the material is determined by two fundamental factors: the electrical conductivity phenomenon within the material (which is mainly dominated by electronic conduction), and the capacitance formed between the CNTs and the cementitious matrix Balberg et al. (1984).

For samples around the percolation threshold (0.2 %*wt* and 0.5 %*wt*), the low CNT concentration allows the CBM to occupy spaces among conductive clusters of CNTs, and hence, many capacitor-type arrangements may be created within the material. As a result, the charge of the formed "capacitors" may cause the electrical polarization phenomena, which is reflected in a constant growth in electrical resistance over time Dong et al. (2016).

In this context, the CNT concentration must be raised to avoid the polarization effect and thus be able to obtain

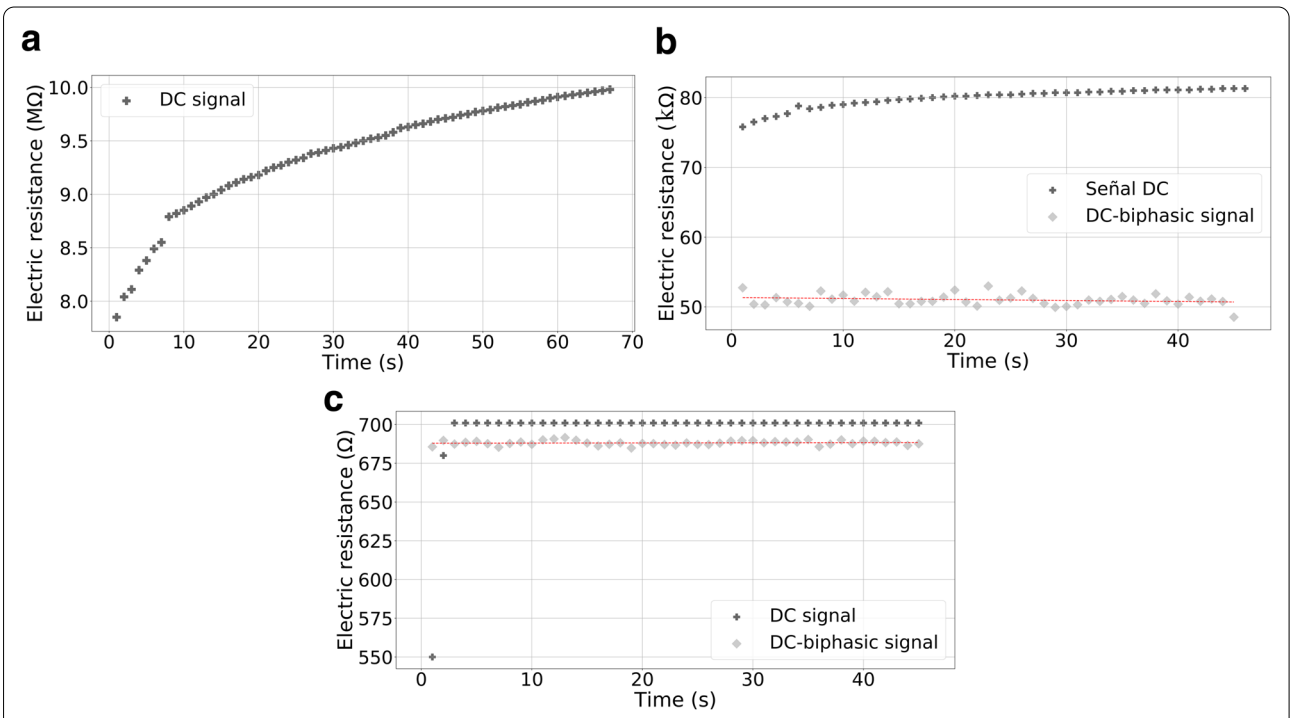

Fig. 9 Comparison using DC and BDC for samples of (**a**) 0.2 %*wt* of CNTs, **b** 0.5 %*wt*, and **c** 0.8 %*wt*.

electrical resistance measurements using DC methods as is seen in samples with 0.8 %*wt* (Fig. 9c), where no electric polarization effect is observed.

As was described in the experimental procedure (Sect. 2.2.3), BDC methodology was performed to avoid polarization phenomena. When analyzing the electrical resistance behavior of the CBM/CNT material characterized by BDC, it is observed that the samples with 0.5 %*wt* (Fig. 9b) do not exhibit electrical polarization phenomena. In other words, their electrical resistance is invariant throughout time, validating in this way, the methodology to avoid the polarization proposed by Downey et al. (2017a), D'Alessandro et al. (2017).

Another aspect that is worth analyzing regarding the results presented in Fig. 9a–c is the magnitude of the electrical resistance. The measurements obtained with DC are higher than the measurements obtained with BDC. This is due to the effect that the electrodes have on the electrical resistance of the material when DC is used. By contrast, when measurements are made with BDC, and the I–V curve method is used, the contribution to the electrical resistance owing to the electrodes is negligible as reported by Konsta-Gdoutos and Aza (2014).

For samples with 0.2 %*wt*, the characterization based on BDC was not carried out due to the low electrical conductivity. When trying to measure the voltage V_{INT}, the characteristic noise signal of the oscilloscope was higher than the magnitude of the voltage, and hence, there was no reliability in the measurements.

3.4 Evaluation of the CBM/CNT Piezoresistive Behavior

In this subsection, the relationship between strain and the change in the electrical resistance of the CBM/CNT material when the samples are subjected to a compression test is established. DC-based methodology was selected to characterize piezoresistive behavior, since the BDC equipment required to measure the composite electrical resistance is a scarce resource, and most are custom-made, resulting in an instrumentation cost increase and hindering industrial scaling.

Also, piezoresistive characterization was only performed on samples which did not exhibit an electrical polarization effect, since it is impractical to wait until the stabilization time of electrical resistance in samples that exhibited electrical polarization, when SHM applications are procured. In this regard, only characterization of the piezoresistive behavior for the sample with 0.8 %*wt* was performed.

The experimental results for the sample with 0.8 %*wt* are shown in Fig. 10. In this figure, the piezoresistive response of the CBM/CNT is observed as repeatable and reversible, since the load does not exceed the CBM/CNT elastic region. In this way, phenomena such as hysteresis

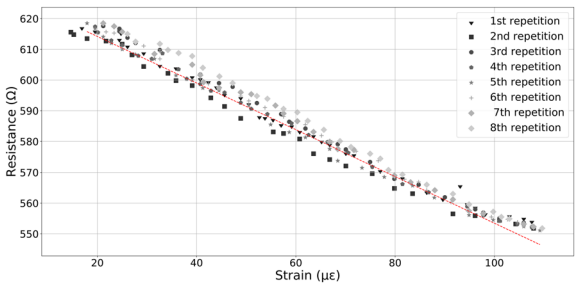

Fig. 10 Piezoresistive phenomenon characterization for sample with 0.8 %*wt* of CNTs.

or variation of the electrical response will not appear due to repeated load application unless a damage occurs.

It is also remarkable the proportionality between the electrical resistance and the compression-induced load. The negative slope in the electric response of the CBM/CNT, when it is subjected to compression loads (due to a negative change in the electrical resistance), is caused by the reduction of the distance among the CNTs D'Alessandro et al. (2017). This behavior makes it easier the implementation of the CBM/CNT for SHM usages Lagason et al. (2016).

Applying Eq. 1 to all the eight repetitions presented in Fig. 10, it was possible to calculate the average gauge factor value ($972.87\epsilon^{-1}$) and its standard deviation ($17.47\epsilon^{-1}$). Based on this result, the repeatability of the CBM/CNT material with 0.8 %*wt* is demonstrated. Besides, it is observed that the CBM/CNT electric resistance starts to vary from the moment when the load is applied, allowing to measure small strain magnitudes.

Observation of Fig. 10 suggests the ability of the CBM/CNT material to withstand strains up to $-100\ \mu\epsilon$ without affecting the structural integrity of the sample, since microcracking or plastic deformation would modify the overall electric resistance and the piezoresistive behavior of the material. This result is in line with the CBM/CNT mechanical characterization carried out following the ASTM C109/C109M-16a and ACI 318-14 standards, where a compressive strength of 30 MPa and a Young's modulus of 20 GPa were determined.

3.5 Health Monitoring of the Reinforced-Concrete Beam Using the CBM/CNT Material

Figure 11 shows the change in the electrical resistance measured in the CBM/CNT material when a load from 0 to 15 kN is applied at a constant displacement speed of 0.5 mm/min. As can be seen, such behavior is nonlinear in the range from 0 to $-10\ \mu\epsilon$. This can be associated with the complex phenomena of load transfer through the different interfaces between the RC-beam

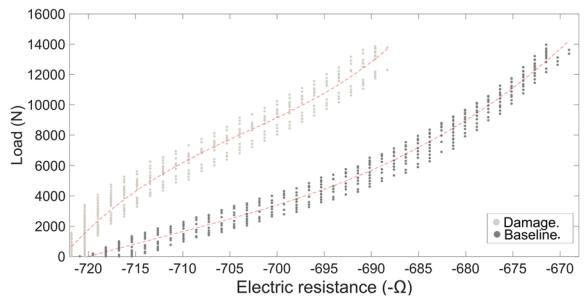

Fig. 11 Behavior of the piezoresistive response of the CBM/CNT against the state of damage and no damage for the RC beam. Dynamic load from 0 to 15 kN.

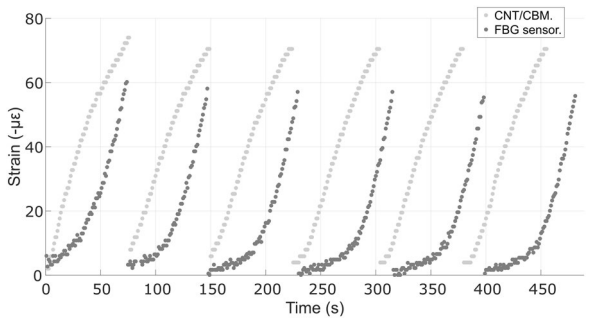

Fig. 12 Behavior of the CBM/CNT and the FBG sensor as a function of time. Dynamic load from 0 to 15 kN.

elements: 1) corrugated steel reinforcement of the RC beam and the concrete of the RC beam, 2) concrete of the RC beam and corrugated steel rods embedded within the parallelepiped (dowels), 3) corrugated steel rods embedded within the parallelepiped (dowels) and CBM/CNT material of the parallelepiped, and finally, 4) steel plate used as positive damage and concrete of the RC beam. In particular, the interface between the steel plate and the concrete was constituted by an epoxy adhesive layer, which could contribute greatly to the appearance of the nonlinear phenomena.

From Fig. 11, it is possible to observe a change in the slope for the damaged state against baseline. Such change can be interpreted as a variation in the global beam stiffness promoted by damage occurrence. This result demonstrates the capability to detect global changes in the stiffness of a simple structure such as a beam by means of strain measurements obtained from a self-sensing concrete. Also, Fig. 11 entails that the CBM/CNT material has the ability to sense small load magnitudes, since the electric resistance experienced a variation associated with small load magnitudes.

To validate the strains obtained through the CBM/CNT parallelepiped embedded into the RC beam, an FBG sensor was bonded to one of the beam sides. Strains measurements were gathered, whilst electrical resistance was measured by using a DC multimeter. The results obtained are presented in Fig. 12.

From Fig. 12, it is possible to observe the repetitiveness of the results obtained for the CBM/CNT material. On the basis of the foregoing, the CBM/CNT as the FBG provided a dynamic response to the load application, wherewith a strain is induced. However, it is observed that there are differences in the strain magnitude as the applied load increases. These differences are mainly due to three factors:

1 The two sensors are not located at the same place (see numbers 4 and 6 in Fig. 6). Therefore, both measurements account for different behaviors at two different locations of the beam,
2 The nonlinear load transfer phenomena as explained in Sect. 2.2.5,

Figure 13 shows the results of the strain measured by the FBG for a dynamic load from 0 to 15 kN at a constant displacement speed of 5 mm/min for the damage and undamaged states. Here, two phenomena can be observed: the first one is the change in slope at low load magnitudes (i.e., loads less than 8kN), whereby it matches with the previously described nonlinear behavior for the load transfer on the RC beam. The second phenomenon is the global change in slope observed when the structure is damaged, compared to the pristine structure.

In contrast to Fig. 13, it is observed that the curves shown in Fig. 11 do not show a significant slope when the applied load is less than 8kN; this is precisely due to the fact that the sensor was embedded within the structure, measuring the strain through a change in its volume; then, it is expected that the behavior of the acquired data is mostly linear as a function of the applied load.

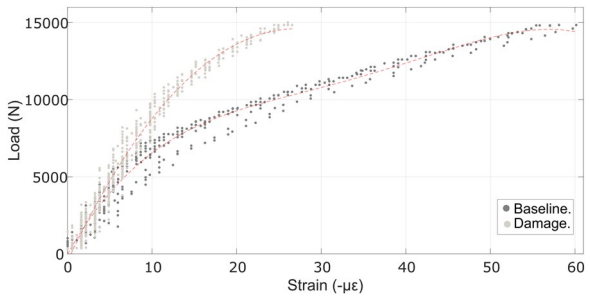

Fig. 13 Behavior of the FBG vs. load for undamaged and damaged conditions.

4 Conclusions

In the present work, the electric and self-sensing properties of a CBM/CNT material were evaluated to determine the feasibility of implementing it as a strain and fault detection sensor. In addition, the piezoresistive behavior of CBM/CNT was evaluated both individually and embedded in a RC beam. The conclusions derived from the present research can be summarized as follows.

1 The dispersion of CNTs within the CBM can be considered as homogeneous for specimens with concentrations of 0.2 %wt, 0.5 %wt, and 0.8 %wt, when using the manufacturing technique presented in this work.
2 The electrical behavior of the CBM/CNT material developed can be described as an ideal resistor; consequently, any method of electrical characterization based on Ohm's law can be used to characterize the electrical resistance. In this way, it is concluded that the most suitable characterization method for electrical resistance is provided by DC methodology. With this method, it is possible to obtain dynamic measurements, the standard deviation is smaller, and experimental setups are simpler and cheaper compared to methods that use a DC-biphasic-type power supply.
3 Electrical polarization phenomenon occurs only when there are low fractions of CNTs and when characterization techniques of the electrical resistance based on the use of a DC source are used, thus, it is concluded that to obtain measurements without electrical polarization, it is necessary to make samples with concentrations of 0.8 %wt or higher. The developed CBM/CNT material shows a dynamic self-sensing response, linear, and repeatable as a function of load application. This makes it attractive for applications in structural health monitoring.
4 The self-sensing response of the CBM/CNT parallelepiped, when is embedded within a civil structure component such as a beam, is similar to the response exhibited by the cubic samples used for characterizing the piezoresistive effect. In both of them, the behavior is linear and repeatable; that is why, the operation of the CBM/CNT material is validated as a strain sensor.
5 It was found that using the CBM/CNT material as a strain sensor, it is possible to infer the damage occurrence in a civil engineering structural component (RC beam) through studying the change of slope in a load–strain curve, which can be associated with a global stiffness change promoted by damage occurrence. This validates the concept of the first SHM stage (damage detection).

Acknowledgements
The authors acknowledge support from Professor Dr. Mónica Lucía AÍvarez-Láinez, in the Department of Product Design Engineering at Universidad EAFIT.

Authors' contributions
DLCS and JSP designed the experiments and geometry samples; DLCS and JAM performed the experiments under the supervision of JSP; DLCS, JSP, and JAM analyzed the data; and DLCS, JSP, JAM, and VMT wrote the paper. All authors read and approved the final manuscript.

Author's information
Mr. Castañeda-Saldarriaga is currently a researcher and professor from Universidad Politécnico Grancolombiano. Castañeda-Saldarriaga completed his Bachelor's degree in physical engineering at Universidad EAFIT and his Master in engineering at Universidad Pontificia Bolivariana. His research interests lie in the area of smart material systems, structural health monitoring, machine learning, artificial intelligent, and deep learning.

Mr. Alvarez-Montoyais currently a Master's degree student at Universidad Pontificia Bolivariana. He has experience in research projects related to structural health monitoring, pattern recognition, machine learning, and composite materials. His current studies focus on smart material systems for renewable energy harnessing.

Dr. Martínez-Tejada is a Bachelor of Science in mechanical engineering from Universidad Pontificia Bolivariana and a Master in materials science and engineering. He pursued his Ph.D. in engineering with a focus on energy and material processing. Martínez-Tejada has made different scientific internships and exchanges in materials science, composite materials, and nanotechnology for energy in INASMET-Spain and CINVESTAV-Mexico.

Dr. Sierra-Pérez currently is a full professor of the Aeronautical Engineering Faculty at Universidad Pontificia Bolivariana, Colombia. He pursued his doctoral studies at Universidad Politécnica de Madrid, Spain, in the Aerospace Engineering Department. His research field is related to composite materials and smart materials in applications of structural health monitoring, nondestructive testing, lightweight structures, and renewable energy.

Funding
The financial support by the Universidad Pontificia Bolivariana (UPB) to the project number 722B-01/17-57, under which the present study is carried out, is acknowledged.

Competing interests
The authors declare that they have no competing interests.

Author details
[1] Grupo de Investigación en Ingeniería Aeroespacial (GIIA), Escuela de Ingenierías, Universidad Pontificia Bolivariana, 050031 Medellín, Colombia. [2] Grupo de Investigación en Nuevos Materiales (GINUMA), Escuela de Ingenierías, Universidad Pontificia Bolivariana, 055030 Medellín, Colombia.

Received: 7 February 2020 Accepted: 28 November 2020
Published online: 19 January 2021

References

ACI Committee 308. (2016). Guide to external curing of concrete. *American Concrete Institute*, page 36. URL https://compass-astm-org.consultaremota.upb.edu.co/DIGITAL_LIBRARY/3PC/5c82c9f3-e27f-484c-94f4-dbbaf9232de3.htm.

Agnisarman, S., Lopes, S., Chalil Madathil, K., Piratla, K., & Gramopadhye, A. (2019). A survey of automation-enabled human-in-the-loop systems for infrastructure visual inspection. *Automation in Construction,97*, 52–76. https://doi.org/10.1016/j.autcon.2018.10.019.

Al-Dahawi, A., Yıldırım, G., Öztürk, O., & Şahmaran, M. (2017). Assessment of self-sensing capability of Engineered Cementitious Composites within the elastic and plastic ranges of cyclic flexural loading. *Construction*

and Building Materials,145, 1–10. https://doi.org/10.1016/j.conbuildmat.2017.03.236. ISSN 09500618.

American Society for Testing and Materials (2014) ASTM C1329/C1329M-12: Standard Specification for Mortar Cement. *ASTM Standard Book*, i:28–31. https://doi.org/10.1520/C1329.

ASTM C109. (2000). Standard Test Method for Compressive Strength of Hydraulic Cement Mortars. *ASTM International, West Conshohocken*, pp.1–6. https://doi.org/10.1520/C0109.

Baeza, F. J., Galao, O., Zornoza, E., & Garcés, P. (2013). Multifunctional cement composites strain and damage sensors applied on reinforced concrete (RC) structural elements. *Materials,6*(3), 841–855. https://doi.org/10.3390/ma6030841. ISSN 19961944.

Balberg, I., Anderson, C. H., Alexander, S., & Wagner, N. (1984). Excluded volume and its realtion to the onset of percolation. *Phsical Review B,30*(7), 3933–3943. https://doi.org/10.1103/PhysRevB.30.3933. ISSN 0163-1829.

Barrias, A., Casas, J. R., & Villalba, S. (2019). Distributed optical fibre sensors in concrete structures: Performance of bonding adhesives and influence of spatial resolution. *Structural Control and Health Monitoring*, 26(3). ISSN 15452255 (ISSN). https://doi.org/10.1002/stc.2310. URL https://www.scopus.com/inward/record.uri?eid=2-s2.0-85058958063&doi=10.1002%2Fstc.2310&partnerID=40&md5=52f48b3df3f1890fcaa298b2f099c01c.

Böttcher, C. J. F. (1973). Polarization and Energy. *Theory of Electric Polarization*, pp. 91–127. Elsevier. ISBN 978-0-444-41019-1. https://doi.org/10.1016/b978-0-444-41019-1.50009-2. URL https://www.sciencedirect.com/science/article/pii/B9780444410191500092.

Castaneda-Saldarriaga, D., Sierra-Perez, J., & Alvarez-Montoya, J. (2019). Synthesis and Characterization of Cement/Carbon-Nanotube Composite for Structural Health Monitoring Applications. In: Proceedings of the 4th World Congress on Civil, Structural, and Environmental Engineering, pp. 1–8. Avestia Publishing. https://doi.org/10.11159/icsect19.149.

Chaoquan, H., Qiao, L., Tian, H., Xianyi, L., Jiang, Q., & Zheng, W. (2011). Role of carbon in the formation of hard Ge1-xCx thin films by reactive magnetron sputtering. *Physica B: Condensed Matter,406*(13), 2658–2662. https://doi.org/10.1016/j.physb.2011.01.077. **ISSN 09214526.**.

Chin, T. S. (2009). Carbon Nanotube Reinforced Composites, volume 3. *ISBN*, *3527408924*, 9783527408924. https://doi.org/10.1016/B978-1-4557-3195-4.00001-1. URL http://books.google.co.uk/books?id=HFe_7Ug9VH4C.

Collins, F., Lambert, J., & Duan, W. H. (2012). The influences of admixtures on the dispersion, workability, and strength of carbon nanotube-OPC paste mixtures. *Cement & Concrete Composites,34*(2), 201–207. https://compass-astm-org.consultaremota.upb.edu.co/DIGITAL_LIBRARY/3PC/5c82c9f3-e27f-484c-94f4-dbbaf9232de3.htm0. **ISSN 0958-9465**.

Coppola, L., Buoso, A., & Corazza, F. (jul 2011) Electrical Properties of Carbon Nanotubes Cement Composites for Monitoring Stress Conditions in Concrete Structures. In: Cadoni, E., & DiPrisco, M. (eds), *Performance, Protection and Strengthening of Structures under Extreme Loading*, volume 82 of *Applied Mechanics and Materials*, pages 118–+. Trans Tech Publications, Ltd., ISBN 978-3-03785-217-0. https://doi.org/10.4028/www.scientific.net/AMM.82.118. URL https://www.amazon.com/Performance-Protection-Strengthening-Structures-Extreme/dp/3037852178?SubscriptionId=AKIAIOBINVZYXZQZ2U3A&tag=chimbori05-20&linkCode=xm2&camp=2025&creative=165953&creativeASIN=3037852178.

Cui, L. (2013). Incorporation of multiwalled carbon nanotubes to ordinary Portland cement (OPC): Effects on mechanical properties. *Biotechnology, Chemical and Materials Engineering Ii, Pts 1 and 2*, 641-642:436–439, . ISSN 1022-6680. https://doi.org/10.4028/www.scientific.net/AMR.641-642.436.

D'Alessandro, A., Pisello, A. L., Sambuco, S., Ubertini, F., Asdrubali, F., Materazzi, A. L., & Cotana, F. (2016b). Self-sensing and thermal energy experimental characterization of multifunctional cement-matrix composites with carbon nanoinclusions. In: Goulbourne, N. C. (ed), *Behavior and Mechanics of Multifunctional Materials and Composites 2016*, volume 9800 of *Proceedings of SPIE*. Spie-Int Soc Optical Engineering, [D'Alessandro, A. Ubertini, F. Materazzi, A. L.] Univ Perugia, Dept Civil & Environm Engn, Perugia, Italy. [Pisello, A. L. Sambuco, Sara Cotana, F.] Univ Perugia, Dept Engn, Perugia, Italy. [Asdrubali, F.] Univ Roma Tre, Dept Engn, Rome, Italy. D'Alessand. ISBN 978-1-5106-0041-6.

D'Alessandro, A., Ubertini, F., García-Macías, E., Castro-Triguero, R., Downey, A., Laflamme, S., Meoni, A., & Materazzi, Annibale, L. (2017) Static and Dynamic Strain Monitoring of Reinforced Concrete Components through Embedded Carbon Nanotube Cement-Based Sensors. *Shock and Vibration*, 2017, ISSN 10709622. https://doi.org/10.1155/2017/3648403.

D'Alessandro, A., Ubertini, F., Laflamme, S., Rallini, M., Materazzi, A. L., Kenny, J. M. (apr 2016c). Strain Sensitivity of Carbon Nanotube Cement-based Composites for Structural Health Monitoring. In: Lynch, J. P. (ed) *Sensors and Smart Structures Technologies for Civil, Mechanical, and Aerospace Systems 2016*, volume 9803 of *Proceedings of SPIE*. SPIE, ISBN 978-1-5106-0044-7. https://doi.org/10.1117/12.2218905.

D'Alessandro, A., Rallini, M., Ubertini, F., Materazzi, A. L., & Kenny, J. M. (2016a). Investigations on scalable fabrication procedures for self-sensing carbon nanotube cement-matrix composites for SHM applications. *Cement & Concrete Composites,65*, 200–213. https://compass-astm-org.consultaremota.upb.edu.co/DIGITAL_LIBRARY/3PC/5c82c9f3-e27f-484c-94f4-dbbaf9232de3.htm2. **ISSN 0958-9465**.

Ding, Y., Liu, G., Hussain, A., Pacheco-Torgal, F., & Zhang, Y. (2019). Effect of steel fiber and carbon black on the self-sensing ability of concrete cracks under bending. *Construction and Building Materials,207*, 630–639. https://compass-astm-org.consultaremota.upb.edu.co/DIGITAL_LIBRARY/3PC/5c82c9f3-e27f-484c-94f4-dbbaf9232de3.htm3.

Dong, S. F., Han, B. G., Ou, J. P., Li, Z., Han, L. Y., & Yu, X. (2016). Electrically conductive behaviors and mechanisms of short-cut super-fine stainless wire reinforced reactive powder concrete. *Cement & Concrete Composites,72*, 48–65. https://compass-astm-org.consultaremota.upb.edu.co/DIGITAL_LIBRARY/3PC/5c82c9f3-e27f-484c-94f4-dbbaf9232de3.htm4. **ISSN 0958-9465**.

Downey, A. R. J., D'Alessandro, A., Ubertini, F., & Laflamme, S. (2018). Crack detection in RC structural components using a collaborative data fusion approach based on smart concrete and large-area sensors. In: Sohn, Hoon (ed) Sensors and Smart Structures Technologies for Civil, Mechanical, and Aerospace Systems,. (2018). *volume 10598, page 123, Department of Mechanical Engineering, Iowa State University, Ames, IA*. United States: SPIE. ISBN 9781510616929. https://doi.org/10.1117/12.2296695. URL https://compass-astm-org.consultaremota.upb.edu.co/DIGITAL_LIBRARY/3PC/5c82c9f3-e27f-484c-94f4-dbbaf9232de3.htm5.

Downey, A., DAlessandro, A., Ubertini, F., Laflamme, S., & Geiger, R. (2017a). Biphasic DC measurement approach for enhanced measurement stability and multi-channel sampling of self-sensing multi-functional structural materials doped with carbon-based additives. *Smart Materials and Structures*, 26(6). ISSN 1361665X. https://doi.org/10.1088/1361-665X/aa6b66.

Downey, A., Alessandro, A. D., Baquera, M., García-macías, E., Rolfes, D., Ubertini, F., et al. (2017). Damage detection, localization and quantification in conductive smart concrete structures using a resistor mesh model. *Engineering Structures,148*, 924–935. https://compass-astm-org.consultaremota.upb.edu.co/DIGITAL_LIBRARY/3PC/5c82c9f3-e27f-484c-94f4-dbbaf9232de3.htm6. **ISSN 0141-0296**.

Eftekhari, M., Hatefi Ardakani, S., & Mohammadi, S. (2014). An XFEM multiscale approach for fracture analysis of carbon nanotube reinforced concrete. *Theoretical and Applied Fracture Mechanics,72*(1), 64–75. https://compass-astm-org.consultaremota.upb.edu.co/DIGITAL_LIBRARY/3PC/5c82c9f3-e27f-484c-94f4-dbbaf9232de3.htm7.

Egemen T. (2015). Measurement of crack length sensitivity and strain gage factor of carbon fiber reinforced cement matrix composites. *Measurement: Journal of the International Measurement Confederation*, 74:21–30, ISSN 02632241. https://doi.org/10.1016/j.measurement.2015.07.021

Elkashef, M. Use of carbon nanotubes in concrete for structural health monitoring—a review. *International Journal of Nanoparticles*, 8(2):99–114, 2015. ISSN 17532507 (ISSN). https://doi.org/10.1504/IJNP.2015.071742. URL https://compass-astm-org.consultaremota.upb.edu.co/DIGITAL_LIBRARY/3PC/5c82c9f3-e27f-484c-94f4-dbbaf9232de3.htm8.

García-Macías, E., Alessandro, A., Castro-Triguero, R., Laflamme, S., Ubertini, F. Enhanced lumped circuit model for smart nanocomposite cement-based sensors under dynamic compressive loading conditions. *Sensors and Actuators A: Physical*, 260:45–57, 2017. ISSN 09244247. https://doi.org/10.1016/j.sna.2017.04.004. URL http://www.sciencedirect.com.recursos.biblioteca.upc.edu/science/article/pii/S0924424717303035 9.

García-Macías, E., Rodríguez-Tembleque, L., Sáez, A., & Ubertini, F. (2018). Crack detection and localization in RC beams through smart MWCNT/epoxy strip-like strain sensors. *Smart Materials and Structures*, 27(11). ISSN 09641726 (ISSN). https://doi.org/10.1088/1361-665X/aae668. URL https://doi.org/10.1016/j.autcon.2018.10.019 0.

Garcia-Macias, E., D'Alessandro, A., Castro-Triguero, R., Perez-Mira, D., & Ubertini, F. (2017). Micromechanics modeling of the uniaxial strain-sensing property of carbon nanotube cement-matrix composites for SHM applications. *Composite Structures,163*, 195–215. https://doi.org/10.1016/j.autcon.2018.10.0191. **ISSN 02638223**.

Glisic, B., Inaudi, D., Lau, J. M., & Fong, C. C. (2013). Ten-year monitoring of high-rise building columns using long-gauge fiber optic sensors. *Smart Materials and Structures*. https://doi.org/10.1016/j.autcon.2018.10.0192.

Gupta, S., Gonzalez, J. G., & Loh, K. J. (2017). Self-sensing concrete enabled by nano-engineered cement-aggregate interfaces. *Structural Health Monitoring,16*(3), 309–323. https://doi.org/10.1016/j.autcon.2018.10.0193. **ISSN 17413168**.

Han, B., Ding, S., & Yu, X. (2015a). Intrinsic self-sensing concrete and structures: A review. Measurement: Journal of the International Measurement Confederation, 59:110–128. ISSN 02632241 (ISSN). https://doi.org/10.1016/j.measurement.2014.09.048. URL https://www.scopus.com/inward/record.uri?eid=2-s2.0-84908053395&doi=10.1016%2Fj.measurement.2014.09.048&partnerID=40&md5=e025e5b982b3a863187be77203b83562.

Hannan, M. A., Hassan, K., & Jern, K. P. (2018). A review on sensors and systems in structural health monitoring: Current issues and challenges. *Smart Structures and Systems*, *22*(5), 509–525. https://doi.org/10.12989/sss.2018.22.5.509. URL: https://www.scopus.com/inward/record.uri?eid=2-s2.0-85058230301&doi=10.12989%2Fsss.2018.22.5.509&partnerID=40&md5=55a9a040cfb7bdd3b5fcbabf315daa695.

Han, B. G., Sun, S. W., Ding, S. Q., Zhang, L. Q., Yu, X., & Ou, J. P. (2015c). Review of nanocarbon-engineered multifunctional cementitious composites. *Composites Part a-Applied Science and Manufacturing,70*, 69–81. https://doi.org/10.1016/j.autcon.2018.10.0196. **ISSN 1359-835X**.

Han, B. G., Wang, Y. Y., Dong, S. F., Zhang, L. Q., Ding, S. Q., Yu, X., et al. (2015b). Smart concretes and structures: A review. *Journal of Intelligent Material Systems and Structures,26*(11), 1303–1345. https://doi.org/10.1016/j.autcon.2018.10.0197. **ISSN 1045-389X**.

Hoseini, A.H.A., Arjmand, M., Sundararaj, U., & Trifkovic, M. (2017). Significance of interfacial interaction and agglomerates on electrical properties of polymer-carbon nanotube nanocomposites. *Materials and Design,125*(April), 126–134. https://doi.org/10.1016/j.autcon.2018.10.0198. **ISSN 18734197**.

Jang, S. H., Hochstein, D. P., Kawashima, S., & Yin, H. M. (2017). Experiments and micromechanical modeling of electrical conductivity of carbon nanotube/cement composites with moisture. *Cement & Concrete Composites,77*, 49–59. **ISSN 0958-9465**.

Kamau, M. N (2012). *Characterisation of multi wall carbon nanotube–polymer composites for strain sensing applications*. PhD thesis, Queensland University of Technology. URL https://doi.org/10.1016/j.conbuildmat.2017.03.2360.

Kang, M.-S. An, Y.-K., Kim, D.-J..Electrical impedance-based crack detection of SFRC under varying environmental conditions. *Smart Structures and Systems*, 22(1):1–11, 2018. ISSN 17381584 (ISSN). https://doi.org/10.12989/sss.2018.22.1.001. URL https://www.scopus.com/inward/record.uri?eid=2-s2.0-85050148278&doi=10.12989%2Fsss.2018.22.1.001&partnerID=40&md5=132bc6ba76d6f3e0a4e20c060df090721.

Kim, G. M., Nam, I. W., Beomjoo Yang, B., Yoon, H. N., & Lee, H. K. and Solmoi Park,. (2019). Carbon nanotube (CNT) incorporated cementitious composites for functional construction materials: The state of the art. *Composite Structures,227*, 111244. https://doi.org/10.1016/j.conbuildmat.2017.03.2362.

Kim, G. M., Yang, B. J., Ryu, G. U., & Lee, H. K. (2016). The electrically conductive carbon nanotube (CNT)/cement composites for accelerated curing and thermal cracking reduction. *Composite Structures,158*, 20–29. https://doi.org/10.1016/j.conbuildmat.2017.03.2363. **ISSN 02638223**.

Konsta-Gdoutos, M. S., & Aza, C. A. (2014). Self sensing carbon nanotube (CNT) and nanofiber (CNF) cementitious composites for real time damage assessment in smart structures. *Cement & Concrete Composites,53*, 162–169. https://doi.org/10.1016/j.conbuildmat.2017.03.2364. **ISSN 0958-9465**.

Konsta-gdoutos, M. S., Metaxa, Z. S., & Shah, S. P. (2010). Cement and Concrete Research Highly dispersed carbon nanotube reinforced cement based materials. *Cement and Concrete Research,40*(7), 1052–1059. https://doi.org/10.1016/j.cemconres.2010.02.0155. ISSN 0008-8846

Kyrylyuk, A. V., & van der Schoot, P. Continuum percolation of carbon nanotubes in polymeric and colloidal media. *Proceedings of the National Academy of Sciences of the United States of America*, 105(24):8221–8226, 2008. ISSN 1091-6490. https://doi.org/10.1073/pnas.0711449105. URL http://www.pnas.org/cgi/content/long/105/24/8221.6.

Lagason, P. H. P., Antonio, O. V. M., & Peneda, S. A. P.. (2016). *Application of carbon nanotubes in structural health monitoring of steel-reinforced concrete*. ISBN 978-1-315-31560-7; 978-1-138-03008-4.

Lee, S., & Park, S. (2017). Composites : Part A Enhanced dispersion and material properties of multi-walled carbon nanotube composites through turbulent Taylor-Couette flow. *Composites Part A,95*, 118–124. https://doi.org/10.1016/j.conbuildmat.2017.03.2367. **ISSN 1359-835X**.

Liao, W.-I., & Chiu, C.-K. (2019). Seismic Health Monitoring of a Space Reinforced Concrete Frame Structure Using Piezoceramic-Based Sensors. *Journal of Aerospace Engineering*. https://doi.org/10.1016/j.conbuildmat.2017.03.2368.

Lim, M. J., Lee, H. K., Nam, I. W., & Kim, H. K. (2017). Carbon nanotube/cement composites for crack monitoring of concrete structures. *Composite Structures,180*, 741–750. https://doi.org/10.1016/j.conbuildmat.2017.03.2369. **ISSN 02638223**.

Liu, C., Liu, G., Ge, Z., Guan, Y., Cui, Z., & Zhou, J. (2019). Mechanical and Self-Sensing Properties of Multiwalled Carbon Nanotube-Reinforced ECCs. *Advances in Materials Science and Engineering*, *1–9*, 2019. https://doi.org/10.1155/2019/2646012. ISSN 1687-8434.

Loh, K. J., & Jesus, G. (2015). Cementitious Composites Engineered with Embedded Carbon Nanotube Thin Films for Enhanced Sensing Performance. *Journal of Physics: Conference Series*, 628(1):12042. ISSN 1742-6588. https://doi.org/10.1088/1742-6596/628/1/012042. URL https://www2.scopus.com/inward/record.uri?eid=2-s2.0-84938718476&doi=10.1088%2F1742-6596%2F628%2F1%2F012042&partnerID=40&md5=88d963eb9c27d7fc89c34c09fd97beb0 http://stacks.iop.org/1742-6596/628/i=1/a=012042?key=crossref.55a4522c8001d14cb34ddce293db825b.

Meo, M. (2014). Acoustic emission sensors for assessing and monitoring civil infrastructures, vol. Elsevier: Amsterdam. ISBN 9780857094322. https://doi.org/10.1533/9780857099136.159.

Meoni, A., D'alessandro, A., Downey, A., García-Macías, E., Rallini, M., Materazzi, A. L. L., Torre, L., Laflamme, S., Castro-Triguero, R., & Ubertini. F. (2018). An experimental study on static and dynamic strain sensitivity of embeddable smart concrete sensors doped with carbon nanotubes for SHM of large structures. *Sensors (Switzerland)*, *18*(3). https://doi.org/10.3390/s18030831. ISSN 14248220 (ISSN). URL https://doi.org/10.3390/ma60308412.

Minot, E. D., Yaish, Y., Sazonova, V., Park, J., Brink, M., & McEuen, Paul L. (2003). Tuning Carbon Nanotube Band Gaps with Strain. *Physical Review Letters,90*(15), 156401. https://doi.org/10.3390/ma60308413. **ISSN 0031-9007**.

Myung, H., Jeon, H., Bang, Y.-S., & Wang, Y. (2014). *Sensor Technologies for Civil Infrastructures*. Elsevier. ISBN 9780857094322. https://doi.org/10.1533/9780857099136.410.

Naeem, F., Lee, H. K., Kim, I., & Nam, W. (2017). Flexural stress and crack sensing capabilities of MWNT/cement composites. *Composite Structures*, *175*, 86–100. https://doi.org/10.1016/j.compstruct.2017.04.078. ISSN 02638223.

Nam, I. W., & Lee, H. K. (2015). Image Analysis and DC Conductivity Measurement for the Evaluation of Carbon Nanotube Distribution in Cement Matrix. *International Journal of Concrete Structures and Materials,9*(4), 427–438. https://doi.org/10.3390/ma60308414. **ISSN 22341315**.

Nešpor, B., & Nejedlík, M. (2018). Development of electrically conductive composite sensors with the addition of functional fillers. *Solid State Phenomena*, 272:34–40. ISSN 1662-9779. https://doi.org/10.4028/www.scientific.net/SSP.272.34. URL https://www2.scopus.com/inward/record.uri?eid=2-s2.0-85043574963&doi=10.4028%2Fwww.scientific.net%2FSSP.272.34&partnerID=40&md5=19bd94f824b31ca1a8e48733f1e008b7.

Noh, Y. J., Pak, S. Y., Hwang, S. H., Hwang, J. Y., Kim, S. Y., & Youn, J. R. (2013). Enhanced dispersion for electrical percolation behavior of multi-walled carbon nanotubes in polymer nanocomposites using simple powder mixing and in situ polymerization with surface treatment of the fillers. *Composites Science and Technology. ISSN*, 02663538, https://doi.org/10.1016/j.compscitech.2013.09.013.

Ogai, H., & Bhattacharya, B. (2018). Smart Sensors for Structural Health Monitoring. URL https://doi.org/10.3390/ma60308417.

PHAM, G.T,. (2008). *Characterization and Modeling of Piezo- Resistive Properties of Carbon Nanotube- Based Conductive Polymer Composites*. PhD thesis.

Pisello, A. L., D'Alessandro, A., Sambuco, S., Rallini, M., Ubertini, F., Asdrubali, F., et al. (2017). Multipurpose experimental characterization of smart nanocomposite cement-based materials for thermal-energy efficiency and strain-sensing capability. *Solar Energy Materials and Solar Cells,161*, 77–88. https://doi.org/10.3390/ma603084118. **ISSN 0927-0248**.

PParvaneh, V., & Khiabani, S. H. (2019). Mechanical and piezoresistive properties of self-sensing smart concretes reinforced by carbon nanotubes. *Mechanics of Advanced Materials and Structures*, 26(11):993–1000. ISSN 15376494 (ISSN). https://doi.org/10.1080/15376494.2018.1432789. URL https://www2.scopus.com/inward/record.uri?eid=2-s2.0-85041522305&doi=10.1080%2F15376494.2018.1432789&partnerID=40&md5=7edea446cec9b763734c2f1b4974ec50.

Qiao, G., Liu, T., Dai, J., Hong, Y., & Wan, J. (2012). Qualitative and quantitative sensors based on electrochemical techniques for the corrosion assessment of RC panels. *IEEE Sensors Journal,12*(6), 2062–2063. https://doi.org/10.1103/PhysRevB.30.39330.

Rana, S., Subramani, P., Fangueiro, R., & Correia, A. G. (2016). A review on smart self-sensing composite materials for civil engineering applications. *AIMS Materials Science*, *3*(2), 357–379. 10.3934/matersci.2016.2.357. URL https://www.scopus.com/inward/record.uri?eid=2-s2.0-85014712628&doi=10.3934%2Fmatersci.2016.2.357&partnerID=40&md5=96e9b0e9d326fc6830c2c8c4e9f8e657.

Rehman, S. K. U., Ibrahim, Z., Jameel, M., Memon, S. A., Javed, M. F., Aslam, M. (2018). Assessment of Rheological and Piezoresistive Properties of Graphene based Cement Composites. *International Journal of Concrete Structures and Materials*, 12(1). ISSN 22341315. https://doi.org/10.1186/s40069-018-0293-0.

Saafi, M. (2009). Wireless and embedded carbon nanotube networks for damage detection in concrete structures. *Nanotechnology*, *20*(39), 7. https://doi.org/10.1088/0957-4484/20/39/395502. ISSN 0957-4484.

Salin, J., Balayssac, J.-P., & Garnier, V. (2018). Introduction. In: *Non-Destructive Testing and Evaluation of Civil Engineering Structures*, pages 1–20. Elsevier. ISBN 9780081023051. https://doi.org/10.1016/B978-1-78548-229-8.50001-7. URL https://linkinghub.elsevier.com/retrieve/pii/B9781785482298500017.

Sarwary, MH., Yıldırım, Gürkan, Al-Dahawi, Ali, Anıl, Özgür, Khiavi, Kaveh A., Toklu, Kenan, & Şahmaran, Mustafa. (jul 2019) Self-Sensing of Flexural Damage in Large-Scale Steel-Reinforced Mortar Beams. *ACI Materials Journal*, 116(4):209–221. ISSN 0889-325X. https://doi.org/10.14359/51715581. URL https://doi.org/10.1103/PhysRevB.30.39334.

Sasmal, S., Ravivarman, N., & Sindu, B. S. (2017). Synthesis, characterisation and performance of piezo-resistive cementitious nanocomposites. *Cement & Concrete Composites,75*, 10–21. https://doi.org/10.1103/PhysRevB.30.39335. **ISSN 0958-9465**.

Schumacher, T., & Thostenson, E. (2014). Development of structural carbon nanotube-based sensing composites for concrete structures. *Journal of Intelligent Material Systems and Structures*, *25*(11):1331–1339. ISSN 1045389X (ISSN). https://doi.org/10.1177/1045389X13505252. URL https://doi.org/10.1103/PhysRevB.30.39336.

Shao, H., Chen, B., Li, B., Tang, S., & Li, Z. (2017). Influence of dispersants on the properties of CNTs reinforced cement-based materials. *Construction and Building Materials,131*, 186–194. https://doi.org/10.1103/PhysRevB.30.39337. **ISSN 09500618**.

Shi, T., Li, Z., Guo, J., Gong, H., & Gu, C. Research progress on CNTs/CNFs-modified cement-based composites – a review. *Construction and Building Materials*, 202:290–307, 2019. ISSN 09500618 (ISSN). https://doi.org/10.1016/j.conbuildmat.2019.01.024. URL https://doi.org/10.1103/PhysRevB.30.39338.

Shull, P. J. (2002). *Nondestructive Evaluation: Theory, Techniques, and Applications*. Mechanical Engineering: CRC Press. ISBN 9780203911068. URL https://doi.org/10.1103/PhysRevB.30.39339.

Sierra-Pérez, J., & Alvarez-Montoya, J. (2020). Strain Field Pattern Recognition for Structural Health Monitoring Applications. In: Tibaduiza-Burgos, Diego Alexander, Anaya-Vejar, Maribel, & Pozo, Francesc (eds) *Pattern Recognition Applications in Engineering*, pages 1–40. IGI Global, Hershey, PA. ISBN 9781799818397. https://doi.org/10.4018/978-1-7998-1839-7.ch001.

Sierra-Pérez, J., Torres-Arredondo, M.-A., & Alvarez-Montoya, J. (2018). Damage detection methodology under variable load conditions based on strain field pattern recognition using FBGs, nonlinear principal component analysis, and clustering techniques. *Smart Materials and Structures. ISSN,1361665X*, https://www.scopus.com/inward/record.uri?eid=2-s2.0-85058958063&doi=10.1002%2Fstc.2310&partnerID=40&md5=52f48b3df3f1890fcaa298b2f099c01c0.

Šimonová, H., Topolár, L., Rovnaník, P., Schmid, P., and Keršner, Z. *Crack initiation of alkali-activated slag based composites with graphite filler*, volume 761 KEM. Trans Tech Publications, Ltd., 2018. ISBN 9783038354406. https://doi.org/10.4028/www.scientific.net/KEM.761.57.

Souri, H., Jaesang, Y., Jeon, H., Kim, J. W., Yang, C. M., You, N. H., et al. (2017). A theoretical study on the piezoresistive response of carbon nanotubes embedded in polymer nanocomposites in an elastic region. *Carbon,120*, 427–437. https://www.scopus.com/inward/record.uri?eid=2-s2.0-85058958063&doi=10.1002%2Fstc.2310&partnerID=40&md5=52f48b3df3f1890fcaa298b2f099c01c1. **ISSN 00086223**.

Sun, X., Song, M. (2009). Conductive behaviour of carbon nanotube based composites. *Doctoral thesis of loughborough university*.

Taheri, S. (2019). A review on five key sensors for monitoring of concrete structures. *Construction and Building Materials,204*, 492–509. https://www.scopus.com/inward/record.uri?eid=2-s2.0-85058958063&doi=10.1002%2Fstc.2310&partnerID=40&md5=52f48b3df3f1890fcaa298b2f099c01c2. **ISSN 09500618**.

Tian Z, Li Y, Zheng J, Wang S & (nov,. (2019). A state-of-the-art on self-sensing concrete: Materials, fabrication and properties. *Composites Part B: Engineering*, *177*, 107437. https://doi.org/10.1016/j.compositesb.2019.107437. ISSN 13598368. URL https://www.scopus.com/inward/record.uri?eid=2-s2.0-85058958063&doi=10.1002%2Fstc.2310&partnerID=40&md5=52f48b3df3f1890fcaa298b2f099c01c3.

Ubertini, F., Laflamme, S., & D'Alessandro, A. (2016). *Smart Cement Paste with Carbon Nanotubes*. Elsevier. ISBN 9781782423447. https://doi.org/10.1016/B978-1-78242-326-3.00006-3.

Ubertini, F., Materazzi, A. L., D'Alessandro, A., & Laflamme, S. (2014). Natural frequencies identification of a reinforced concrete beam using carbon nanotube cement-based sensors. *Engineering Structures,60*, 265–275. https://www.scopus.com/inward/record.uri?eid=2-s2.0-85058958063&doi=10.1002%2Fstc.2310&partnerID=40&md5=52f48b3df3f1890fcaa298b2f099c01c4. **ISSN 0141-0296**.

Wang, Y., Xue, C., Ding, S., Zhang, C., & Han, B. (2015). Force analysis of self-sensing cement-based sensors embedded in concrete. *Jianzhu Cailiao Xuebao/Journal of Building Materials*. https://www.scopus.com/inward/record.uri?eid=2-s2.0-85058958063&doi=10.1002%2Fstc.2310&partnerID=40&md5=52f48b3df3f1890fcaa298b2f099c01c5.

Xu, Y.-L., & Jia. H (apr 2017). *Smart civil structures*. CRC Press, Department of Civil and Environmental Engineering, Faculty of Construction and Environment, The Hong Kong Polytechnic University, Hong Kong. ISBN 9781498743990 (ISBN); 9781498743983 (ISBN). https://doi.org/10.1201/9781315368917.

Xu, J., Butler, L. J., & Elshafie, M. Z. E. B. (2019). Experimental and numerical investigation of the performance of self-sensing concrete sleepers. *Structural Health Monitoring,*. https://doi.org/10.1177/1475921719834506.

Yamazaki, F., Ueda, H., & Liu, W. (2018). Basic study on detection of deteriorated rc structures using infrared thermography camera. *Engineering Journal,22*(3), 233–242. https://www.scopus.com/inward/record.uri?eid=2-s2.0-85058958063&doi=10.1002%2Fstc.2310&partnerID=40&md5=52f48b3df3f1890fcaa298b2f099c01c7.

Yang, Q., Liu, P., Ge, Z., & Wang, D. (2020). Self-sensing carbon nanotube-cement composite material for structural health monitoring of pavements. *Journal of Testing and Evaluation*, 48(3). ISSN 00903973 (ISSN). 10.1520/JTE20190170. URL https://www.scopus.com/inward/record.uri?eid=2-s2.0-85058958063&doi=10.1002%2Fstc.2310&partnerID=40&md5=52f48b3df3f1890fcaa298b2f099c01c8.

Yıldırım, G., Sarwary, MH, Al-Dahawi, A., Öztürk, O, Anıl, Ö, & Şahmaran, M. (2018). Piezoresistive behavior of CF- and CNT-based reinforced concrete beams subjected to static flexural loading: Shear failure investigation. *Construction and Building Materials*, 168:266–279. ISSN 09500618. https://doi.org/10.1016/j.conbuildmat.2018.02.124.

Yoo, D.-Y., Kim, S., & Lee, S. H. (2018). Self-sensing capability of ultra-high-performance concrete containing steel fibers and carbon nanotubes under tension. *Sensors and Actuators, A: Physical,276*, 125–136. https

://www.scopus.com/inward/record.uri?eid=2-s2.0-85058958063&doi=10.1002%2Fstc.2310&partnerID=40&md5=52f48b3df3f1890fcaa298b2f099c01c9.

Yorke, R. (1981). Chapter 4 - Circuit Analysis. Yorke, R., (ed), *Electric Circuit Theory*, pages 200–235. Pergamon. ISBN 978-0-08-026133-1. https://doi.org/10.1016/B978-0-08-026133-1.50011-5. URL http://www.sciencedirect.com/science/article/pii/B9780080261331500115.

You, I., Yoo, D.-Y., Kim, S., Kim, M.-J., & Zi, G. (2017). Electrical and self-sensing properties of ultra-high-performance fiber-reinforced concrete with carbon nanotubes. *Sensors (Switzerland)*. https://www.sciencedirect.com/science/article/pii/B97804444101915000921.

Zhao, G., Zhang, D., Zhang, L., & Wang, B. (2018). Detection of defects in reinforced concrete structures using ultrasonic nondestructive evaluation with piezoceramic transducers and the time reversal method. *Sensors (Switzerland)*. https://www.sciencedirect.com/science/article/pii/B9780444410191500092 2.

Publisher's Note